NJC
Letter

Selective hydrogenation of adiponitrile over a Raney Ni–P amorphous catalyst†

Hexing Li,[a,b] **Yeping Xu**[b] **and Jing-Fa Deng***[a]

[a] *Department of Chemistry, Fudan University, Shanghai 200433, P. R. China*
E-mail: ifdeng@srcap.stc.sh.cn
[b] *Department of Chemistry, Shanghai Normal University, Shanghai 200234, P. R. China.*

Received (in Montpellier, France) 14th September 1999, Accepted 17th September 1999

A Raney Ni–P amorphous catalyst, prepared by alkali leaching of an amorphous Ni–Al–P alloy obtained by the rapid quenching technique, exhibited excellent activity and selectivity toward 1,6-hexanediamine during the gas–solid phase hydrogenation of adiponitrile at 1 atm pressure.

The hydrogenation of adiponitrile (ADN) into 1,6-hexanediamine (HMA) is one of the key transformations in the manufacturing of Nylon-6,6.[1–3] In industry, the hydrogenation is performed in a liquid phase at high pressure, in which Raney Ni and Raney Co are probably the most frequently used catalysts.[4–7] Large quantities of ammonia are found to be essential to decrease side reactions leading to secondary and tertiary amines, presumably due to the presence of a diimine intermediate.[4,8] The gas–solid phase hydrogenation of ADN at 1 atm pressure over Ni/Al_2O_3 catalysts was recently reported by Sueiras *et al.*[9–11] Although these supported Ni catalysts exhibited high activity, their selectivity toward HMA was very poor (less than 40%). As is well known, amorphous alloys represent a new class of materials with short-range ordering structure that may provide pathways to novel, more active and selective catalysts in various hydrogenation processes.[12–16] In earlier times, these materials (typically, Ni–P amorphous alloy) were usually prepared by the rapid quenching technique.[17–20] However, their industrial application is still quite limited due to their extremely low surface area (*ca.* 1.0 $m^2\ g^{-1}$) and poor thermal stability since the amorphous structure is thermodynamically metastable.

In this communication, an attempt has been made to develop a novel Ni–P amorphous alloy catalyst with a pronounced skeletal structure like Raney Ni (denoted as Raney Ni–P). Its catalytic performance was investigated during the gas–solid hydrogenation of ADN at 1 atm pressure, in the absence of ammonia. The as-prepared Raney Ni–P exhibited excellent selectivity, similar to that of the regular Ni–P amorphous alloy catalyst, but its activity was much higher. In comparison with other Ni-based catalysts, including crystallized Raney Ni–P, $Ni/\gamma\text{-}Al_2O_3$, and Raney Ni, Raney Ni–P exhibited much higher selectivity to HMA at 100% conversion of ADN.

The Raney Ni–P sample was prepared by the following procedure. A mixture containing 48.2 wt% metallic Ni, 48.7 wt% metallic Al and 3.1 wt% red P was melted at 1673 K in an argon atmosphere. The melted solution was then cooled rapidly ($10^6\ K\ s^{-1}$) by the rapid quenching technique[21] using a single steel roll at a very high stirring rate (2500 rpm), resulting in Ni–Al–P amorphous alloy in the form of ribbons *ca.* 5 mm wide and 10–20 μm thick. Then, 6.0 g of the as-prepared Ni–Al–P sample was ground to 200 mesh powder and added very slowly over a 1.5 h period into 60 ml of 6.0 M NaOH solution at 273 K. The alkali leaching was carried out at 343 K for 6.0 h in an N_2 atmosphere with vigorous stirring. The resulting sample was then washed clean of alkali and aluminates with H_2O (until pH = 7 was obtained). It was further washed with ethanol (EtOH) to remove water, and finally, stored under EtOH. Raney Ni catalyst was prepared by alkali leaching a commercially available crystalline Ni–Al alloy (Ni : Al 50 : 50 w/w) using a similar procedure. Crystalline Raney Ni–P was obtained by treating the fresh Raney Ni–P sample at 673 K for 2 h in N_2 flow. Regular Ni–P amorphous alloy was prepared by the rapid quenching technique from the melted solution containing only metallic Ni and red P, as described by Yamashita *et al.*[18] Ni/Al_2O_3 was prepared according to the method described by Sueiras *et al.*[10] with $\gamma\text{-}Al_2O_3$ (BET area, 190 $m^2\ g^{-1}$) as the support.

The bulk composition of the as-prepared catalysts was determined by inductively coupled plasma (ICP) analysis. The BET surface area and the pore volume of the catalysts were determined by N_2 adsorption at 77 K using an ASAP 2010 (Micro-meritics). The active surface area was measured by H_2 chemisorption, assuming H/Ni(s) = 1 and a surface area of $6.5 \times 10^{-20}\ m^2$ per Ni atom, based on an average of the areas for the (100), (110) and (111) planes. According to Table 1, one can see the presence of a pronounced pore volume in Raney Ni–P, similar to that in Raney Ni, which could account for its higher surface area than that of regular Ni–P. The lower surface area of the crystalline Raney Ni–P indicates the coalescense of small particles during the pretreatment at high temperature. Although a large BET surface area and pore volume were measured for $Ni/\gamma\text{-}Al_2O_3$ its relatively low active surface area demonstrates that the surface active Ni atoms are not as well-dispersed as those in the Raney Ni–P and Raney Ni samples.

Table 1 Some characteristics of the as-prepared catalyst samples

Catalyst	Composition/atom %	$S_{BET}/m^2\ g^{-1}$	$V_{pore}/ml\ g^{-1}$	$S_{act}/m^2\ g^{-1}$
Raney Ni–P	$Ni_{68}Al_{25}P_7$	87	0.050	38
Regular Ni–P	$Ni_{88}P_{12}$	1.2	–[a]	0.8
Crystalline Raney Ni–P	$Ni_{69}Al_{26}P_5$	57	0.028	15
Raney Ni	$Ni_{68}Al_{32}$	106	0.070	43
30 wt% $Ni/\gamma\text{-}Al_2O_3$	Ni	135	0.072	14

[a] Not measurable.

The amorphous character of the Raney Ni–P sample was determined by X-ray powder diffraction (XRD, Rigaku Dmax-3C with Cu-Kα radiation). As shown in Fig. 1(*a*) only one broad peak around $2\theta = 45°$ was observed in the XRD pattern, similar to that found for the regular Ni–P amorphous alloy,[15–17] indicating a typical amorphous character. When the sample was treated at 673 K for 2 h in N_2 flow, various sharp peaks corresponding to metal Ni, crystalline Ni–Al alloy and Ni–P alloy were observed, as shown in Fig. 1(*b*), indicating crystallization of the Ni–P amorphous alloy at high temperature. In addition, the appearance of the diffractional peaks of crystalline Ni–P alloy in the XRD pattern indicates the presence of the metallic Ni–P alloy in the fresh Raney Ni–P sample since no significant Ni–P alloy diffractional peaks were observed in the XRD pattern of the mixture containing metallic Ni and red P when it was treated under the same conditions. The amorphous structure of Raney Ni–P was further confirmed by the extended X-ray absorption fine structure (EXAFS, BL-10B). Fig. 2(*a*) shows the radial distribution functions (RDF) of the fresh sample obtained from the $\chi(k)k^3$ Ni edge by fast Fourier transformation. Only one broad peak around $R = 2.1$ Å was observed, indicating that the sample has no long-range order but only a short-range ordering structure confined within the first near-neighbor atom layer.[22] After the sample was treated at 673 K, a remarkable increase in the strength of the original peak and two additional small peaks at longer distances (*ca.* 3.7–4.6 Å) were observed, as shown in Fig. 2(*b*) indicating a transformation from the amorphous structure to a well-ordered crystalline structure. Differential scanning calorimetry (DSC, Perkin-Elmer) also revealed that the Raney Ni–P sample was thermodynamically metastable and underwent an exothermic crystallization at 670 K. However, the crystallization temperature of Raney Ni–P is nearly 70 K higher than that of regular Ni–P, demonstrating the great improvement of its thermal stability by the skeletal structure and the presence of residual Al species.

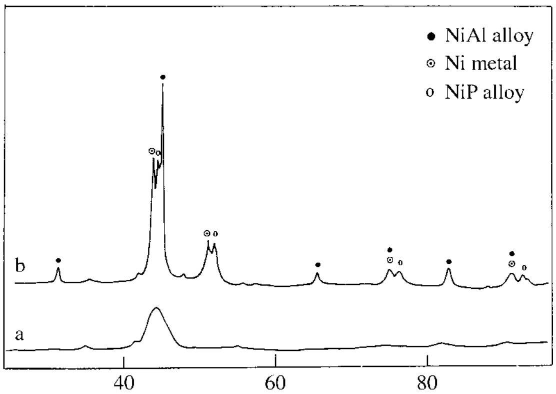

Fig. 1 XRD patterns of Raney Ni–P samples: (*a*) fresh, (*b*) after being treated at 673 K for 2.0 h.

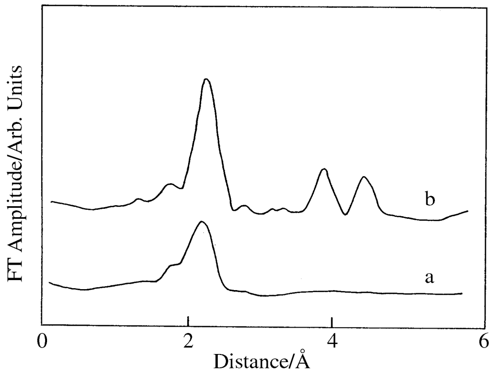

Fig. 2 RDF curves of Raney Ni–P samples: (*a*) fresh, (*b*) after being treated at 673 K for 2.0 h.

The surface electronic state of Raney Ni–P was determined by X-ray photoelectron spectroscopy (XPS, Perkin-Elmer PH I 5000C). All binding energy (BE) values were calibrated by using the BE value of contaminant carbon ($C_{1S} = 284.6$ eV) as a reference. Fig. 3 shows the XPS spectra of a Raney Ni–P sample, before and after Ar^+ etching for 600 s. The XPS spectra in the Al_{2P} level demonstrates that most of the Al species are present in the oxidized state (BE = 74.3 eV) throughout the catalyst. In the $Ni_{2P_{3/2}}$ level, two peaks around BE values of 852.7 eV and 856.2 eV represent metallic Ni in Ni–P(Al) alloy (denoted as Ni^0) and oxidized Ni (denoted as Ni^{ox}), respectively. The Ni^{ox} species disappeared after Ar^+ etching, showing that in the bulk of the sample, almost all the Ni species are present as Ni^0. In contrast, both the P in Ni–P alloy (P^0, BE = 129.6 eV) and the oxidized P (P^{ox}, BE = 133.4 eV) species were observed in the P_{2P} level with or without Ar^+ etching, indicating that P was oxidized in the bulk. In comparison with the standard BE values of metallic Ni and red P, no significant BE shift of either Ni^0 or P^0 was observed, indicating that the electronic interaction between Ni and P in the Ni–P alloy could be neglected.

The activity test was carried out in a tubular glass fixed-bed reactor (0.8 cm ID) in a continuous process at 1 atm pressure (473 K), and in the absence of ammonia. The reaction conditions are as follows: catalyst amount = 1.0 g, space velocity = 1700 h^{-1}, H_2 : ADN = 37 (molar ratio). Our preliminary study revealed that the catalyst did not show diffusion restrictions under the present conditions. The ADN dissolved in EtOH was vaporized in a bubbling-type evaporator at 523 K, and then fed into the reactor with a hydrogen mixture as carrier gas (75 ml min^{-1}). The effluents were analyzed by means of an on-line gas chromatograph (GC 1102) with a flame ionization detector equipped with a 25 m OV 101 capillary column, and a 353–533 K oven temperature programmed as a 4 K min^{-1} ramp. Conversion and selectivity were defined by the following equations: conversion (%) = (mol of ADN consumed) × 100/(mol of ADN fed). Selectivity (%) = (mol of HMA determined) × 100/(mol of ADN consumed).

The metallic Ni species in the Ni–P alloy were proven to be the active sites in the ADN hydrogenation by the following observations. (1) No significant activity was observed when Raney Ni–P was preoxidized in an O_2 flow at 503 K for 2.0 h while the high activity was recovered after it was reduced in a H_2 flow for another 2.0 h. (2) The initial activity of Raney Ni–P was relatively poor and then increased gradually during the reaction. This can be understood by considering that oxidized Ni species cover the catalyst surface, as shown by the XPS spectra in Fig. 3, and that these can be gradually reduced under H_2 flow during the reaction. After 3 h, constant activity and selectivity were obtained, indicating that the catalyst

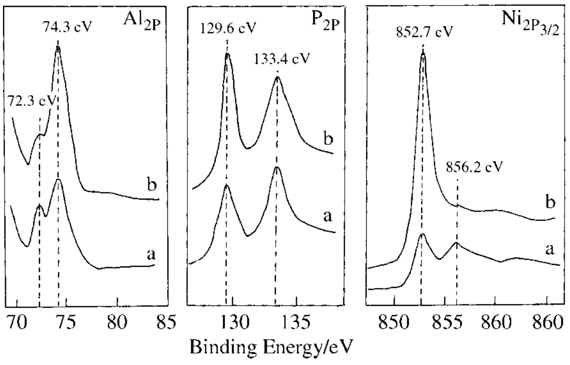

Fig. 3 XPS spectra of a Raney Ni–P sample: (*a*) original, (*b*) after etching for 600 s.

Table 2 Catalytic behavior of different catalysts[a]

Catalyst	Conversion(%)	Selectivity(%)		
		HMA	6-Aminohexanenitrile	Azacycloheptane
Raney Ni–P	100	64	21	15
Regular Ni–P	17	65	25	10
Crystalline Raney Ni–P	100	15	78	7
Raney Ni	100	5	87	8
30 wt % Ni/γ–Al_2O_3	100	27	16	53

[a] Reaction conditions: fixed-bed reactor, catalyst amount = 1.0 g, space velocity = 1700 h^{-1}, H_2/ADN = 37 (molar ratio), $P = 1$ atm, $T = 473$ K.

reached a steady state. All the catalytic activities and selectivities mentioned in the following discussion were collected during the steady state.

As shown in Table 2, all the Ni-based catalysts, except the regular Ni–P amorphous alloy, exhibited very high activities (100% conversion of ADN) under the reaction conditions used. The lower activity of the regular Ni–P is possibly attributed to its extremely low surface area. By GC various products have been identified and it was found that the nature of the catalyst strongly influenced the product distribution. Raney Ni–P and regular Ni–P favor HMA formation, Raney Ni and crystalline Raney Ni–P are responsible for 6-aminohexanenitrile formation, while Ni/γ-Al_2O_3 tends to produce azacycloheptane. Therefore, we can indicate the order of selectivity to HMA as Raney Ni–P ≈ regular Ni–P > Ni/γ-Al_2O_3 > crystalline Raney Ni–P > Raney Ni.

As is well known, there are several factors affecting the selectivity of the catalyst. Thus, the high selectivity of Ni/γ-Al_2O_3 to azacycloheptane is presumably attributed to the strong interaction between Ni active sites and the γ-Al_2O_3 support.[11] The similar selectivity of Raney Ni–P to that of regular Ni–P is attributed to their similar amorphous structures. Raney Ni–P and regular Ni–P amorphous catalysts exhibit much higher selectivity to HMA than crystalline Raney Ni–P or Raney Ni, implying that the amorphous structure plays an important role in determining the distribution of the reaction products in the present ADN hydrogenation, which is usually interpreted in terms of electronic and structural effects. As no significant electronic interaction between Ni and P was observed, the higher selectivity of Raney Ni–P to HMA is mainly attributed to the unique structural characteristics of the Ni active sites in the Ni–P amorphous alloy, owing to the modification of alloying P since the XPS results reveal a P enrichment on the surface of the Raney Ni–P catalyst.

To confirm the above conclusion, the structural parameters of Ni active sites were calculated from the EXAFS data. As shown in Table 3, one can see that the parameters of both Raney Ni–P and regular Ni–P amorphous alloys are almost the same, while they are quite different from those of either crystalline Raney Ni–P or crystalline Raney Ni. The relatively lower coordination number (N) demonstrates that the Ni atoms in Raney Ni–P and regular Ni–P amorphous alloy are more highly unsaturated. The relatively higher Debye–Waller factor (σ), which represents the disordering degree, reveals that the Ni active sites are distributed more homogeneously in the aforementioned Ni–P amorphous alloys. As pointed out by Baiker in his review on metallic glasses as catalysts,[13] these structural properties favor excellent selectivities in hydrogenation reactions. Its should be noted that detailed studies on the reaction mechanism of ADN hydrogenation and of the absorption of ADN and the reaction intermediates on different catalysts should be performed to elucidate the above results. These studies are underway.

Table 3 Structural parameters of the Ni-based catalysts

Catalyst	$R_{Ni–Ni}$/Å	N	σ/Å
Raney Ni–P	2.48	4.0	0.61
Regular Ni–P	2.49	4.0	0.60
Crystalline Raney Ni–P	2.52	6.0	0.50
Raney Ni	2.51	5.5	0.49
Ni foil	2.50	12	–

This work was supported by the National Natural Science Foundation of China and SINOPEC. We also owe all our thanks to Shanghai Education Committee for its financial support.

Notes and references

† Non-SI units employed: 1 atm ≈ 101 kPa; 1 eV ≈ 9.65 J mol^{-1}.

1 K. Weissermel and H.-J. Arpe, *Industrial Organic Chemistry*, VCH, Weinheim, 2nd edn., 1993.
2 A. Baiker, J. De Pietro, M. Maciejewski and B. Walz, *Stud. Surf. Sci. Catal.*, 1991, **67**, 169.
3 B. Torok, A. Molnar, K. Borszeky, E. Toth-Kadar and I. Bakonyi, *Stud. Surf. Sci. Catal.*, 1993, **78**, 179.
4 C. de. Bellefon and P. Fouilloux, *Catal. Rev.-Sci. Eng.*, 1994, **36**, 459.
5 J. L. Dallons, G. Jannes and B. Delmon, *Acta Chim. Hung.*, 1985, **119**, 223.
6 J. A. Schreifels, P. C. Maybury and W. E. Swartz, Jr., *J. Org. Chem.*, 1981, **46**, 1263.
7 D. Gavroy, C. Joly-Vuillemin, G. Cordier, P. Fouilloux and H. Delmas, *Catal. Today*, 1995, **24**, 103.
8 R. L. Augustine, *Catal. Rev.-Sci. Eng.*, 1976, **13**, 285.
9 F. Medina, P. Salagre and J. E. Sueiras, *J. Mol. Catal.*, 1993, **81**, 363.
10 F. Medina, P. Salagre and J. E. Sueiras, *J. Chem. Soc., Faraday Trans. 1*, 1993, **89**, 3507.
11 F. Medina, P. Salagre and J. E. Sueiras, *J. Chem. Soc., Faraday Trans. 1*, 1994, **90**, 1455.
12 M. Shibata and T. Masumoto, *Prep. Catal.*, 1987, **4**, 353.
13 A. Baiker, *Faraday Discuss. Chem. Soc.*, 1989, **87**, 239.
14 A. Molnar, G. V. Smith and M. Bartok, *Adv. Catal.*, 1989, **36**, 329.
15 J. F. Deng, H. Li and W. J. Wang, *Catal. Today*, 1999, **51**, 113.
16 Y. Chen, *Catal. Today*, 1998, **44**, 3.
17 S. Yoshida, H. Yamashita, T. Funabiki and T. Yonezawa, *J. Chem. Soc., Chem. Commun.*, 1982, 964.
18 S. Yoshida, H. Yamashita, T. Funabiki and T. Yonezawa, *J. Chem. Soc., Faraday Trans. 1*, 1984, **80**, 1435.
19 H. Yamashita, T. Funabiki and S. Yoshida, *J. Chem. Soc., Chem. Commun.*, 1984, 868.
20 H. Yamashita, M. Yoshikawa, T. Funabiki and S. Yoshida, *J. Chem. Soc., Faraday Trans. 1*, 1985, **81**, 2485.
21 B. N. Zong, E. Z. Min and Y. S. Zhu, *CN Pat.*, 1073726A, 1993.
22 J. A. Schwarz, C. Contescu and A. Contescu, *Chem. Rev.*, 1995, **95**, 477.

Paper 9/07467H